
Refiner: Refining Self-attention for Vision Transformers

Daquan Zhou, Yujun Shi, Bingyi Kang, Weihao Yu,
Zihang Jiang, Yuan Li, Xiaojie Jin, Qibin Hou, Jiashi Feng

National University of Singapore
{zhoudaquan21, andrewhou, weihaoyu6, xjjin0731}@gmail.com
{jzihang, kang, shi.yujun}@u.nus.edu, elefjia@nus.edu.sg

Abstract

Vision Transformers (ViTs) have shown competitive accuracy in image classification tasks compared with CNNs. Yet, they generally require much more data for model pre-training. Most of recent works thus are dedicated to designing more complex architectures or training methods to address the data-efficiency issue of ViTs. However, few of them explore improving the self-attention mechanism, a key factor distinguishing ViTs from CNNs. Different from existing works, we introduce a conceptually simple scheme, called *refiner*, to directly refine the self-attention maps of ViTs. Specifically, *refiner* explores *attention expansion* that projects the multi-head attention maps to a higher-dimensional space to promote their diversity. Further, *refiner* applies convolutions to augment local patterns of the attention maps, which we show is equivalent to a *distributed local attention*—features are aggregated locally with learnable kernels and then globally aggregated with self-attention. Extensive experiments demonstrate that *refiner* works surprisingly well. Significantly, it enables ViTs to achieve 86% top-1 classification accuracy on ImageNet with only 81M parameters. Code is publicly available at https://github.com/zhoudaquan/Refiner_ViT.

1 Introduction

Recent progress on image classification largely attributes to the development of vision transformers (ViTs) [19, 48, 49]. Unlike convolutional neural networks (CNNs) that rely on convolutions (*e.g.*, using 3×3 kernels) to process features locally [46, 25, 41, 65, 58], ViTs take advantage of the self-attention (SA) mechanism [51] to establish the global-range relation among the image patch features (*a.k.a.* tokens) and aggregate them across all the spatial locations. Such global information aggregation nature of SA substantially increases ViT’s expressiveness and has been proven to be more flexible than convolutions [45, 48, 60, 27, 34] on learning image representations. However, it also leads ViTs to need extraordinarily larger amount of data for pre-training (*e.g.*, JFT-300M) or much longer training time and stronger data augmentations than its CNN counterparts to achieve similar performance [48].

Most of recent works thus design more complex architectures or training methods to improve data-efficiency of ViTs [48, 60, 45]. However, few of them pay attention to the SA component of ViTs. Within a SA block in ViTs, each token is updated by aggregating the features from *all* tokens according to the attention maps, as shown in Fig. (1)(b). In this way, the tokens of a layer are able to sufficiently exchange information with each other and thus offer great expressiveness. However, this can also cause different tokens to become more and more similar, especially as the model goes deeper (more information aggregation). This phenomenon, also known as over-smoothing, has been identified by some recent studies [66, 49, 18] to largely degrade the performance of the ViTs.

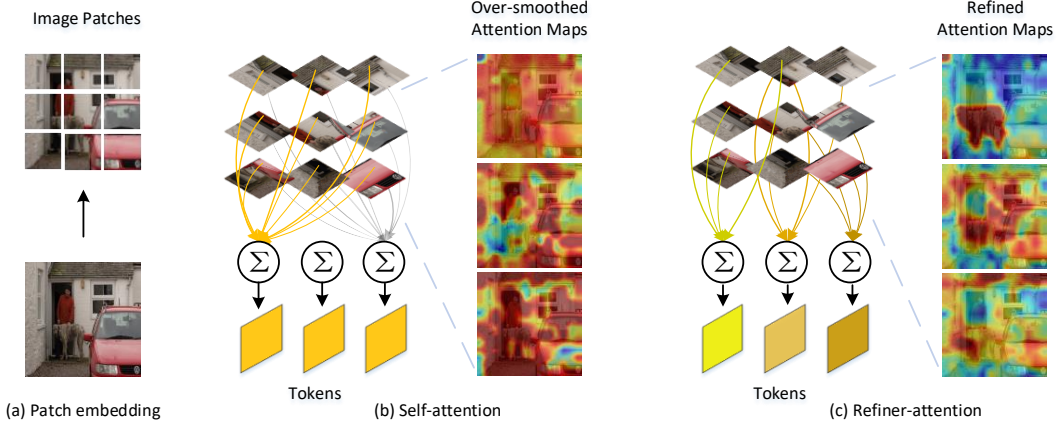


Figure 1: Illustration on our motivation. (a) The input image is regularly partitioned into patches for patch embedding. (b) The token-wise attention maps from vanilla self-attention of ViTs tend to be uniform, and thus they aggregate all the patch embeddings densely and generate overly-similar tokens. (c) Differently, our proposed refiner augments the attention maps into diverse ones with enhanced local patterns, such that they aggregate the token features more selectively and the resulting tokens are distinguishable from each other.

In this work, we explore to address the above limitation by directly refining their self-attention maps. Specifically, inspired by the recent works [49] demonstrating that increasing the number of SA heads can effectively improve the model performance, we investigate how to promote the diversity of the attention maps using a similar strategy. However, given a transformer model with fixed embedding dimension, directly increasing the number of heads will reduce the number of embeddings allocated to each head, making the computed attention map less comprehensive and accurate as shown in Tab. 9 in [49]. To address this dilemma, we explore *attention expansion* that linearly projects the multi-head attention maps to a higher-dimensional space spanned by a larger number of attention maps. As such, the number of attention heads (used for computing the attention maps) are implicitly increased without reducing the embedding dimension per head, enabling the model to enjoy both benefits from more SA heads and high embedding dimension.

Additionally, we argue that ignoring the local relationship among the tokens is another main cause of the above mentioned over-smoothing issue of global SA. The locality (local receptive fields) and spatial invariance (weight sharing) have been proven to be the key of the success of CNNs across many computer vision tasks [31, 44, 53, 25, 1]. Therefore, we explore how to leverage the convolution to augment the attention mechanism of ViTs. Some recent works have studied injecting convolutional locality into ViTs, *e.g.*, integrating both convolution and global self-attention into a hybrid model [19, 45]. However, they mostly consider directly applying convolution to the token features, keeping the convolutional block and the SA block separately. Differently, we explore introducing convolution to the attention maps directly to augment their spatial-context and local patterns, thus increasing their diversity. Such an approach, as we explain later, can be understood as a *distributed local attention* mechanism that combines both strengths of self-attention (global-range modeling) and convolution (reinforcing local patterns).

Based on the above two strategies, we introduce the *refiner* scheme to directly enhance self-attention maps within ViTs. Though being conceptually simple, it works surprisingly well. As shown in Fig. 1(c), the attention map with refiner has preciser focus on the target object, compared to the vanilla one. By directly applying refiner to the SA module, the performance of the ViT-Base [19] is improved by 1.7% on ImageNet under the same training recipes with negligible memory overhead (less than 1M). We have experimentally verified that this improvement is consistent when using more complex training recipes [48, 49] and the results are shown in Appendix. Surprisingly, refiner is also applicable for natural language processing tasks. On GLUE [52], it increases the average score by 1% over the state-of-the-art BERT [16].

In summary, our contributions are: First, we tackle the important low data-efficiency issue of ViTs from a new angle, *i.e.*, directly refining the self-attention maps. We investigate a simple yet novel

refiner scheme and find it works surprisingly well, even outperforming the state-of-the-art methods using sophisticated training recipes or leveraging extra models. Secondly, the introduced refiner makes several interesting modifications on the self-attention mechanism that would be inspiring for future works. Its attention expansion gives a new viewpoint for addressing the common dilemma on the trade-off between the number of attention heads and the embedding dimensions. Besides, different from the common practice that applies convolutions to features, it proves that convolutions can effectively augment attention maps as well and improve the model performance significantly.

2 Related Works

Transformers for vision tasks Transformers [51] were originally developed for solving natural language processing tasks and achieved remarkable success [5, 38]. Different from other deep neural network architectures like CNNs and RNNs [33, 40], transformers rely on the self-attention mechanism to perform the global interactions among features instead of relying on certain inductive biases (*e.g.*, locality and weight sharing from CNNs). This grants transformers stronger capacity in learning from large-scale data. Those properties of transformers motivate researchers to explore its application on computer vision tasks, including image enhancement [9, 59], image classification [19, 60, 66], object detection [6, 68, 13, 64], segmentation [54, 34, 64], video processing [62, 67] and 3D point cloud data processing [63, 22]. Among them, Vision Transformer (ViT) [19] is one of the early pure-transformer based models that achieve state-of-the-art performance on ImageNet. However, due to the larger model capacity, ViTs need extraordinarily large-scale datasets (*e.g.*, ImageNet-22K and JFT-300M) for pre-training to achieve comparable performance with CNNs at similar model size. Some follow-up models thus try to resolve the low data-efficiency limitation either by modifying the model architecture [60, 48, 49] or adopting new training techniques like knowledge distillation [48].

Injecting locality into ViTs Recent works find that injecting the convolution locality into transformer blocks can boost performance of ViTs. As initially proposed in [19, 45], the hybrid ViT uses pre-trained CNN models to extract the patch embedding from the input images and then deploys multiple transformer blocks for feature processing. [32] replaces the feed forward block in the transformer block with an inverted residual one [41, 26] and [37] propose to build two concurrent branches: one with convolution and the other one with transformer. However, they all leverage convolutions to strengthen the features. Besides, the interaction between the global information aggregation at the SA block and the local information extraction in the convolution block is not well explored. In this paper, we focus on enhancing the attention maps and explore how the global context and the local context can be combined in a novel way.

3 Refiner

3.1 Preliminaries on ViT

The vision transformer (ViT) first tokenizes an input image by regularly partitioning it into a sequence of n small patches. Each patch is then projected into an embedding vector x_i via a linear projection layer, with an additional learnable position embedding.

Then ViT applies multiple multi-head self-attention (MHSA) and feedforward layers to process the patch embeddings to model their long-range dependencies and evolve the token embedding features. Suppose the input tensor is $X \in \mathbb{R}^{d_{in} \times n}$, the MHSA applies linear transformation with parameters W_K, W_Q, W_V to embed them into the key $K = W_K X \in \mathbb{R}^{d \times n}$, query $Q = W_Q X \in \mathbb{R}^{d \times n}$ and value $V = W_V X \in \mathbb{R}^{d \times n}$ respectively. Suppose there are H self-attention heads. These embeddings are uniformly split into H segments $Q_h, K_h, V_h \in \mathbb{R}^{d/H \times n}$. Then the MHSA module computes the head-specific attention matrix (map)¹ A and aggregate the token value features as follows:

$$\text{Attention}(X, h) = A^h V_h^\top \text{ with } A^h = \text{Softmax} \left(\frac{Q_h^\top K_h}{\sqrt{d/H}} \right), h = 1, \dots, H. \quad (1)$$

¹We interchangeably use attention matrix and attention map to call A when the context is clear. Specifically, the attention matrix means the original A while the attention map means reshaped A to the input size.

Limitations of ViTs The ViT purely relies on the global self-attention to establish the relationship among all the tokens without deploying any spatial structure priors (or inductive biases). Though benefiting in learning flexible features from large-scale samples, such global-range attention may lead to overly-smoothed attention maps and token features as pointed out by [66, 21]. We hypothesize this may slow the feature evolving speed of ViTs, *i.e.*, the features change slowly when traversing the model blocks, and make the model perform inferior to the ones with faster feature evolving speed. To verify this, we present a pilot experiment to compare the feature learning speed of ViTs with similar-size CNNs (ResNet) [25] that incorporate strong locality regularization and DeiT [48] which is a better-performing transformer model trained with sophisticated scheme.

In Fig. 2, we plot the CKA similarity [28] (ref. its formula to Appendix) between the intermediate token features at the output of each block and the final output, normalized by the similarity between the first and final layer features. Such a metric captures two properties: how fast the intermediate features converge to the final features and how much the final features are different from the first layer features. It is clearly shown that for the ViT, the feature evolves slowly after the first several blocks. Differently, the token features of ResNet and DeiT keep evolving faster when the model goes deeper and the final features are more different than the first layer features compared with the ViT. In this work, we investigate whether such limitation of ViTs can be solved by refining the attention maps into more diverse and locality-aware ones.

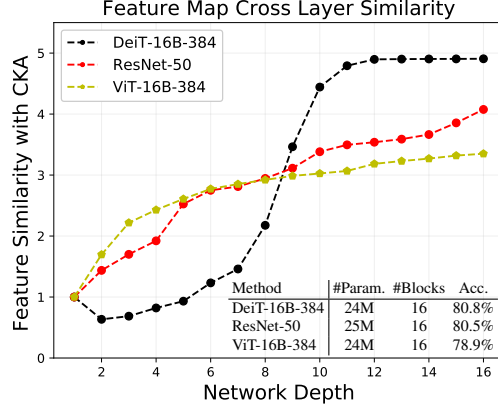


Figure 2: The features of ViT evolves slower than ResNet [25] and DeiT [48] across the model blocks.

3.2 Attention Expansion

The MHSA of transformers captures different aspects of the input features [51] by projecting them into different subspaces and computing self-attention therein. Thus, increasing the number of attention heads within MHSA, which is shown to be effective at improving the model performance [49], can potentially increase diversity among the attention maps. However, as mentioned above, if naively adding more SA heads, for a model with fixed hidden dimension, it is difficult to trade-off the benefit of having more SA heads and the harm of reducing the embedding dimension per head.

To resolve this issue, instead of directly expanding the attention heads, we investigate expanding the number of self-attention maps via linear transformation. Concretely, we use a linear projection $W_A \in \mathbb{R}^{H' \times H}$ with $H' > H$ to project the attention maps $\mathbf{A} = [A^1; \dots; A^H]$ to a new set of attention maps $\tilde{\mathbf{A}} = [\tilde{A}^1, \dots, \tilde{A}^{H'}]$ with $\tilde{A}^h = \sum_{i=1}^H W_A(h, i) \cdot A^i, h = 1, \dots, H'$. Then we use the new attention maps $\tilde{\mathbf{A}}$ to aggregate features as in Eqn. (1).

The above attention expansion implicitly increases the number of SA heads but does not sacrifice the embedding dimensions. To understand how it works, recall each of the original SA map A_h is computed by $A_h = Q_h^\top K_h$. Here we omit the softmax and normalizing factor for illustration simplicity. We use w_i to denote $W_A(h, i)$. Thus, the up-projected attention map is computed by $\tilde{A}^h = \sum_{i=1}^H w_i \cdot Q_i^\top K_i = [w_1 \cdot Q_1, \dots, w_H \cdot Q_H]^\top K$. Different from the vanilla MHSA that divides Q, K into H sub-matrices for SA computation, the attention expansion reweighs the Q features with learnable scalars and uses the complete reweighed Q to compute the SA maps. Getting rid of the feature division, the attention expansion effectively solves the above issue. When only one weight scalar is non-zero, it degenerates to the vanilla MHSA. The attention expansion is similar to the talking-heads attention [42, 66] which are proven effective in improving attention diversity but differently, it expands the number of attention maps while talking-heads does not change the number.

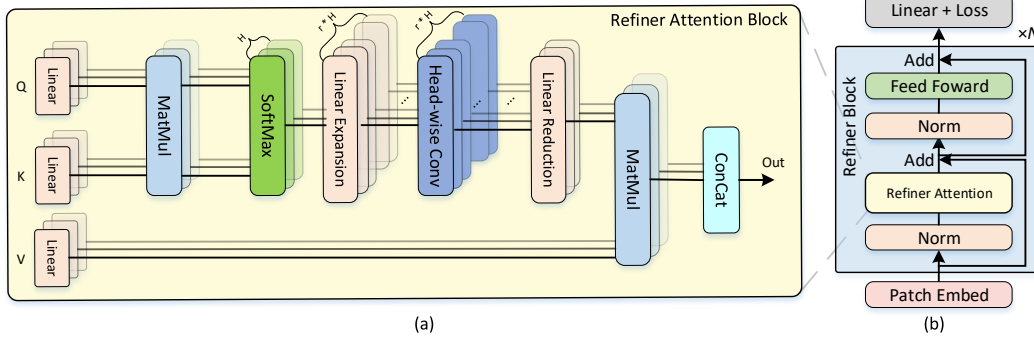


Figure 3: (a) Architecture design of refiner. Different from the vanilla self-attention block, the refiner applies linear attention expansion to attention maps output from the softmax operation to increase their number. Then head-wise spatial convolution is applied to augment these expanded attention maps. Finally another linear projection is deployed to reduce the number of attention maps to the original one. Note that $r = H'/H$ is the expansion ratio. (b) Modified transformer block with refiner as a drop-in component.

3.3 Distributed Local Attention

Our second strategy is to investigate how convolutions can help enhance self-attention maps since convolutions are good at strengthening local patterns. Different from some earlier trials on introducing convolutions to process features in ViTs [45, 32, 37], we explore directly applying convolutions to the self-attention maps.

Given the pre-computed self-attention matrix A^h from head h , we apply a learnable convolution kernel $\mathbf{w} \in \mathbb{R}^{k \times k}$ of size $k \times k$ to modulate it as follows:

$$A_{i,j}^{h*} = \sum_{a,b=1}^k \mathbf{w}_{a,b} \cdot A_{i-\lfloor \frac{k}{2} \rfloor + a, j-\lfloor \frac{k}{2} \rfloor + b}^h.$$

Then the standard SA-based feature aggregation as Eqn. (1) is conducted with this new attention matrix $\tilde{\mathbf{v}}_i = \sum_{j=1}^n \tilde{A}_{i,j}^* \cdot \mathbf{v}_j$.

Though being conceptually simple, the above operation establishes an interesting synergy between the global context aggregation (with self-attention) and local context modeling (with convolution). To see this, consider applying 1D convolution \mathbf{w} of length k to obtain the convolution-augmented SA matrix, with which the feature aggregation becomes

$$\begin{aligned} \tilde{\mathbf{v}}_i &= \sum_{j=1}^n A_{i,j}^{h*} \cdot \mathbf{v}_j = \sum_{j=1}^n \left(\sum_{a=1}^k \mathbf{w}_a \cdot A_{i,j-\lfloor \frac{k}{2} \rfloor + a}^h \right) \cdot \mathbf{v}_j \\ &= \sum_{j=1}^n \left(\sum_{a=1}^k \mathbf{w}_a \cdot A_{i,j-\lfloor \frac{k}{2} \rfloor + a}^h \cdot \mathbf{v}_j \right) = \sum_{j=1}^n \left(\sum_{a=1}^k A_{i,j}^h \cdot \mathbf{w}_a \cdot \mathbf{v}_{j-a+\lfloor \frac{k}{2} \rfloor} \right). \end{aligned}$$

The above clearly shows that the feature aggregation based on the convolution-processed attention matrix is equivalent to: (1) applying the convolution \mathbf{w} , with a location-specific reweighing scalar $A_{i,j}^h$, to aggregate features locally at first and (2) summing over the locally aggregated features. Therefore, we name such an operation as *distributed local attention* (DLA).

We empirically find DLA works pretty well in the experiments. We conjecture that DLA effectively combines strengths of the two popular feature aggregation schemes. Convolutional schemes are strong at capturing local patterns but inefficient in global-range modeling. Moreover, stacking multiple convolutions may suffer the increasingly center-biased receptive field [35], leading the model to ignore the features at the image boundary. In contrast, self-attention based feature aggregation can effectively model the global-range relation among features but suffer the over-smoothing issue. DLA can effectively overcome their limitations and better model the local and global context jointly.

3.4 Refiner and Refined-ViT

The attention expansion and distributed local attention can be easily implemented via 1×1 and 3×3 convolutions. Fig. 3 illustrates the refiner architecture. Different from the vanilla self-attention, refiner expands the attention maps at first and then applies head-wise convolution to process the maps. Refiner additionally introduces the attention reduction for reducing the model computation cost and maintaining the model embedding dimension. Specifically, similar to attention expansion, the attention reduction applies linear projection to reduce the number of attention maps from H' to the original H , after the distributed local attention. Refiner can serve as a drop-in module to directly replace the vanilla self-attention in each ViT transformer block, giving the *Refined-ViT* model.

4 Experiments

4.1 Experiment Setup

We mainly evaluate Refiner for the image classification task. Besides, we also conduct experiments on natural language processing tasks to investigate its generalizability to NLP transformer models.

Computer vision We evaluate the effectiveness of the refiner on ImageNet [15]. For a fair comparison with other methods, we first replace the SA module with refiner on ViT-Base [19] model as it is the most frequently used one [19, 48, 61, 49]. When comparing with other state-of-the-art methods, we modify the number of transformer blocks and the embedding dimensions to increase the efficiency in the same manner as [60, 66].

Natural language processing We evaluate our model on the General Language Understanding Evaluation (GLUE) benchmark [52]. GLUE benchmark includes various tasks which are formatted as single sentence or sentence pair classification. See Appendix for more details of all tasks. We measure accuracy for MNLI, QNLI, QQP, RTE, SST, Spearman correlation for STS and Matthews correlation for CoLA. The GLUE score is the average score for all the 8 tasks.

Training setup All the experiments are conducted upon PyTorch [36] and the timm [56] library. The models are trained on ImageNet-1k from scratch without auxiliary dataset. For the ablation experiments, we follow the standard training schedule and train our models on the ImageNet dataset for 300 epochs. When compared to state-of-the-art (SOTA) models, we use the advanced training recipes as proposed in [48]. Detailed training hyper-parameters are listed in the appendix.

4.2 Analysis

Refiner introduces attention expansion and convolutional local kernels to augment the self-attention maps of ViTs. Here we individually investigate their effectiveness through ablative studies.

Table 1: Effect of the expansion ratio in attention expansion, which varies from 1 to 6. The model is Refined-ViT with 16 blocks, 12 attention heads and 384 embedding dimension.

Expan. Ratio	Params	Converge (#Epoch)	Top-1 (%)
1	25M	300	82.3
2	25M	300	82.8
3	25M	273	82.8
4	25M	270	82.9
6	25M	261	83.0

Effect of attention expansion We adopt 1×1 convolution to adjust the number of attention maps. In this ablative study, we vary the expansion ratio $r = H'/H$ from 1 to 6. From the results in Tab. 1, we observe that along with increased expansion ratio (and more attention maps), the model performance monotonically increases from 82.3% to 83.0%. This clearly demonstrates the effectiveness of attention expansion in improving the model performance. Note when the expansion ratio equals to 1, the attention expansion degenerates to the talking-heads attention [42, 66]. Compared with this strong baseline, increasing the ratio to 2 brings 0.5% top-1 accuracy improvement. Interestingly, using larger expansion ratio speeds up the convergence of model training. Using an expansion ratio of 6 saves the number of training epochs by nearly 13% (261 vs. 300 epochs). This

Table 2: Impacts of convolution on attention maps. We directly apply the 3×3 convolution on the attention maps from the multi-head self-attention of ViTs with respect to various architectures. We can observe clear improvement for all ViT variants when adding the proposed DLA.

Model	#Blocks	Hidden dim	#Heads	Params	Top-1 (%)
ViT	12	768	12	86M	79.5
+ DLA	12	768	12	86M	81.2
ViT	16	384	12	24M	78.9
+ DLA	16	384	12	24M	80.3
ViT	24	384	12	36M	79.3
+ DLA	24	384	12	36M	80.9
ViT	32	384	12	48M	79.2
+ DLA	32	384	12	48M	81.1

Table 3: Effect of attention reduction on Refined-ViT-16B with 384 hidden dimension.

Model	Attn. map	Top-1 (%)
Refined-ViT-16B w/o reduction		82.99
Refined-ViT-16B w/ reduction		82.95

Table 4: Evaluation on how the spatial span within DLA affects the model performance. We compare the model performance with three different constraints on the local kernels.

Model	Constraints	Top-1 (%)
Refined-ViT-16B	None	83.0
Refined-ViT-16B	Spatial	82.7
Refined-ViT-16B	Row+Col	81.7

reflects that attention expansion can help the model learn the discriminative token features faster. However, when the expansion ratio is larger than 3, the benefits in the model accuracy attenuates. This motivates us to explore the distributed local attention for further performance enhancement.

Effect of attention reduction Refiner deploys another 1×1 convolution to reduce the number of attention maps from H' to the original number H , after the attention expansion and distributed local attention, in order to reduce the computation overhead due to expansion. We conduct experiments to study whether reduction will hurt model performance. As observed from Tab. 3, attention reduction drops the accuracy very marginally, implying the attention maps have been sufficiently augmented in the higher-dimension space.

Effect of distributed local attention We then evaluate whether the distributed local attention (DLA) works consistently well across a broad spectrum of model architectures. We evaluate its effectiveness for various ViTs with 12 to 32 SA blocks, without the attention expansion. Following the common practice [19], the hidden dimension is 768 for the ViT-12B and 384 for all the other ViTs. We set the local attention window size as $k = 3$ and use the DLA to replace all the self-attention block within ViT. From the results summarized in Tab. 2, DLA can consistently boost the top-1 accuracy of various ViTs by 1.2% to 1.7% with negligible model size increase. Such significant performance boost clearly demonstrates its effectiveness and the benefits brought by its ability in jointly modeling the local and global context of input features. The combined effects of attention expansion and DLA are shown in Tab. 7.

Effect of the local attention kernels Refiner directly applies the 3×3 convolution onto the attention maps A . We compare this natural choice with another two feasible choices for the local kernels. The first one is to apply spatially adjacent convolution on the reshaped attention maps such that the aggregated tokens by the local kernels are spatially adjacent in the original input. Specifically, we reshape each row of A into a $\sqrt{n} \times \sqrt{n}$ matrix² which together form a $\sqrt{n} \times \sqrt{n} \times n$ tensor and apply 3×3 convolution. The second one is to apply the combination of row and column 1D convolution. From the results in Tab. 4, we find the spatially adjacent convolution will slightly hurt the performance while only adopting the 1D convolution leads to 1.3% accuracy drop. Directly applying convolution to the attention maps (as what refiner does)

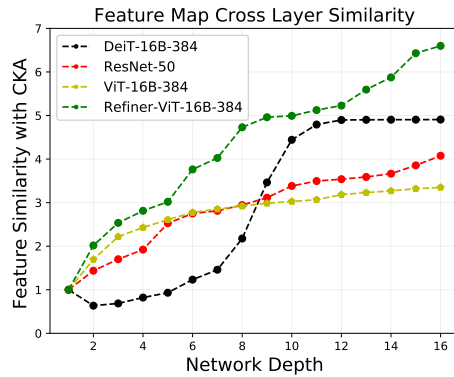


Figure 4: Refiner accelerates feature evolving compared with CNNs, the vanilla ViT and the Deit trained with a more complex scheme.

²Recall n is the number of tokens and the input image is divided into $\sqrt{n} \times \sqrt{n}$ patches.

gives the best performance, demonstrating the effectiveness of augmenting the local patterns of the attention maps.

Refiner augments attention maps and accelerates feature evolving We visualize the attention maps output from different self-attention blocks without and with the refiner in Fig. 5. Clearly, the attention maps after Refiner become not so uniform and present stronger local patterns. We also plot the feature evolving speed in Fig. 4, in terms of the CKA similarity change w.r.t. the first block features and Refined-ViT evolves the features much faster than ViTs.

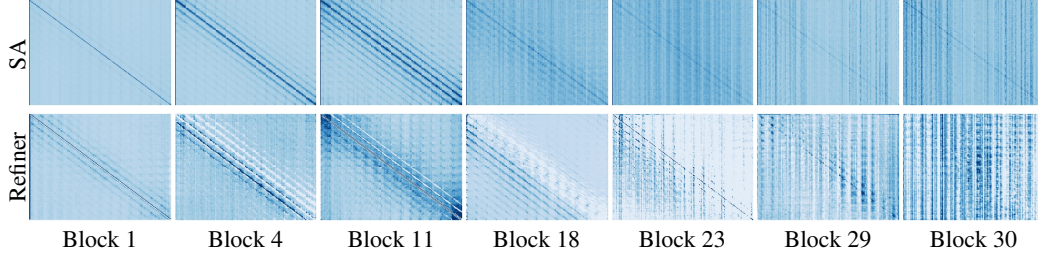


Figure 5: Compared with the attention matrices A from the vanilla SA (top), for deeper blocks, refiner (bottom) strengthens the local patterns of their attention maps, making them less uniform and better model local context.

4.3 Comparison with SOTA

We compare refined-ViT with state-of-the-art models in Tab. 7. For small-sized model, with 224×224 test resolution, Refined-ViT-S (with only 25M parameters) achieves 83.6% accuracy on ImageNet, which outperforms the strong baseline DeiT-S by 3.7%. For medium-sized model with 384×384 test resolution, the model Refined-ViT-M achieves the accuracy of 85.6%, which outperforms the latest SOTA CaiT-S36 by 0.2% with 13% less of parameters (55M vs. 68M) and outperforms LV-ViT-M by 1.6%. Note that CaiT uses knowledge distillation based method to improve their model, requiring much more computations. For large-sized model finetuned with input resolution of 448×448 , refined-ViT achieves 86%, better than CaiT-M36 with 70% less of parameters (81M vs. 271M). This is the new state-of-the-art results on ImageNet with less than 100M parameters. Notably, as shown in Tab. 7, our models significantly outperform the recent models that introduce locality into the token features across all the model sizes. This clearly demonstrates: first, refining the attention maps (and thus the feature aggregation mechanism) is more effective than augmenting the features for ViTs; secondly, jointly modeling the local and global context (from DLA in the refiner) is better than using the convolution and self-attention separately and deploying them into different blocks.

4.4 Receptive field calibration

In this subsection, we present and investigate a simple approach that we find can steadily improve classification performance of ViT. The approach is a generic one that also works well for CNNs.

As pointed out in [50], pre-processing the training images and testing images separately could lead to a distribution shift between the training and testing regimes. This issue has been named by [50] as the mismatch between the region of classification (RoC), which could degrade performance of the classification model. A common remedy solution is to apply random cropping to get a centrally cropped image patch for classification, with a certain cropping ratio (less than 1), at the testing phase. However, as the receptive field of a deep neural network at the deep layers is typically larger than the image size, we argue that it is not necessary to crop a patch from the testing images.

Instead, we propose to pad the testing image such that all the image features can be captured by the model. Different from directly feeding the image into the model, padding the image with zeros can align the informative region of an image to the center of the receptive field of the model, similar to random cropping, while getting rid of information loss. Thus it can further improve the model accuracy. We name this padding method as *receptive field calibration* (RFC). RFC can be easily implemented by setting the cropping ratio to be larger than 1, which we call it *RFC ratio*, during the testing phase.

To investigate its effectiveness, among all the models whose pre-trained weights are publicly available, we apply RFC on the top 2 accurate CNN models and ViTs respectively. The results are summarized in Tab. 5. It is observed that RFC can easily further improve the performance of current SOTA model by 0.11% *without* fine-tuning. It is worth noting that the selected models are pre-trained with large auxiliary datasets such as ImageNet-22k and JFT-300M and the performance is nearly saturated. The testing image resolutions vary from 384 to 800. Under a variety of model configurations, RFC consistently improve the accuracy. With RFC, our proposed Refined-ViT achieves a new SOTA on the ImageNet (among models with less than 100M parameters).

It should be noted that in the above experiments (Sec. 4.2 and 4.3), including comparing Refined-ViT with SOTAs, we did *not* apply RFC for fair comparisons. Here we would like to share such RFC technique as an interesting finding from our recent experiments. RFC is a generic and convenient technique to improve model’s classification performance. We believe it is inspiring for rethinking the common random cropping techniques. More importantly, it motivates future studies to dig into the effect of the model’s receptive field in classification performance and explore how to calibrate it w.r.t. the input images to gain better performance.

Table 5: RFC can improve both CNN and ViT-based SOTA models on ImageNet, outperforming the strategy of random cropping. We apply RFC on the best performing pre-trained models available online. RFC improves the top-1 accuracy consistently across a wide spectrum of models and configurations, and establishes the new SOTA on ImageNet.

Model	Rand Crop. Ratio	Top-1 (%)	RFC Ratio	Top-1 (%)
EfficientNet-l2-ns-800 [46]	0.960	88.35	1.120	88.46
EfficientNet-b7-ns-475 [46]	0.936	88.23	1.020	88.33
Swin-large-patch4-w12-384 [34]	1.000	87.15	1.100	87.18
CaiT-m48-448 [21]	1.000	86.48	1.130	86.56
Refined-ViT-448	1.000	85.94	1.130	85.98

4.5 Applied to NLP tasks

We also evaluate the performance of Refiner-ViT models for natural language processing tasks on the GLUE benchmark, to investigate whether Refiner also improves other transformer-based models. We use the BERT-small [11] as the baseline model and replace the self-attention module with refiner, using the same pre-training dataset and recipes. From the results in Tab. 6, Refiner boosts the model performance across all the tasks significantly and increases the average score by 1%, demonstrating Refiner is well generalizable to transformer-based NLP models to improve their attentions and final performance.

Table 6: Comparison of BERT-small w/o and w/ refiner on the GLUE development set.

Model	Params	MNLI	QNLI	QQP	RTE	SST	MRPC	CoLA	STS-B	Avg.
BERT-small [11]	14M	75.8	83.7	86.8	57.4	88.4	83.8	41.6	83.6	75.1
+ Refiner	14M	78.1	86.4	88.0	57.6	88.8	84.1	42.2	84.0	76.1

5 Conclusions

In this work, we introduced the refiner, a simple scheme that augments the self-attention of ViTs by attention expansion and distributed local attention. We find it works surprisingly well for improving performance of vision transformers (ViT). Furthermore, it also improves the performance of NLP transformers (BERT) by a large margin. Though refiner is limited to improving diversity of the self-attention maps, we believe its working mechanism is also inspiring for future works on understanding and further improving the self-attention mechanism.

Some interesting questions arise from the empirical observations but we leave them open for future studies. First, traditionally all the elements within the attention maps are normalized to be between 0 and 1. However, the attention expansion does not impose such a constraint while giving quite

Table 7: Top-1 accuracy comparison with other methods on ImageNet [15] and ImageNet Real [3]. All models are trained without external data. With the same computation and parameter constraint, Refined-ViT consistently outperforms other SOTA CNN-based and ViT-based models. The results of CNNs and ViT are adopted from [49].

Network	Params	FLOPs	Train size	Test size	Top-1(%)	Real Top-1 (%)
CNNs						
EfficientNet-B5 [46]	30M	9.9B	456	456	83.6	88.3
EfficientNet-B7 [46]	66M	37.0B	600	600	84.3	—
Fix-EfficientNet-B8 [46, 50]	87M	89.5B	672	800	85.7	90.0
NFNet-F0 [4]	72M	12.4B	192	256	83.6	88.1
NFNet-F1 [4]	133M	35.5B	224	320	84.7	88.9
Transformers						
ViT-B/16 [19]	86M	55.4B	224	384	77.9	83.6
ViT-L/16 [19]	307M	190.7B	224	384	76.5	82.2
T2T-ViT-14 [60]	22M	5.2B	224	224	81.5	—
T2T-ViT-14 \uparrow 384 [60]	22M	17.1B	224	384	83.3	—
CrossViT [8]	45M	56.6B	224	480	84.1	—
Swin-B [34]	88M	47.0B	224	384	84.2	—
TNT-B [24]	66M	14.1B	224	224	82.8	—
DeepViT-S [66]	27M	6.2B	224	224	82.3	—
DeepViT-L [66]	55M	12.5B	224	224	83.1	—
DeiT-S [48]	22M	4.6B	224	224	79.9	85.7
DeiT-B [48]	86M	17.5B	224	224	81.8	86.7
DeiT-B \uparrow 384 [48]	86M	55.4B	224	384	83.1	87.7
CaiT-S36 \uparrow 384 [49]	68M	48.0B	224	384	85.4	89.8
CaiT-M36 [49]	271M	53.7B	224	224	85.1	89.3
LV-ViT-S [27]	26M	6.6B	224	224	83.3	88.1
LV-ViT-M [27]	56M	16.0B	224	224	84.0	88.4
Transformer with locality						
LocalViT-S [32]	22.4M	4.6B	224	224	80.8	-
LocalViT-PVT [32]	13.5M	4.8B	224	224	78.2	-
ConViT-S [14]	27M	5.4B	224	224	81.3	-
ConViT-S+ [14]	48M	10.0B	224	224	82.2	-
BoTNet-S1-59 [45]	33.5M	7.3B	224	224	81.7	-
BoTNet-S1-110 [45]	54.7M	10.9B	224	224	82.8	-
BoTNet-S1-128 [45]	79.1M	19.3B	256	256	84.2	-
BoTNet-S1-128 \uparrow 384 [45]	79.1M	45.8B	256	384	84.7	-
Our Refined-ViT						
Refined-ViT-S	25M	7.2B	224	224	83.6	88.3
Refined-ViT-S \uparrow 384	25M	24.5B	224	384	84.6	88.9
Refined-ViT-M	55M	13.5B	224	224	84.6	88.9
Refined-ViT-M \uparrow 384	55M	49.2B	224	384	85.6	89.3
Refined-ViT-L	81M	19.1B	224	224	84.9	89.1
Refined-ViT-L \uparrow 384	81M	69.1B	224	384	85.7	89.7
Refined-ViT-L \uparrow 448	81M	98.0B	224	448	85.9	90.1

good results. It is worthy future studies on the effects of such subtraction attention (with negative attention weights) for feature aggregation. Second, the local distributed attention indeed imposes a locality inductive bias which is proven to be effective in enhancing learning efficiency of ViTs from medium-sized datasets (ImageNet). How to automatically learn the suitable inductive biases would be another interesting direction and some recent works have started to explore [14].

References

- [1] Irwan Bello. Lambdanetworks: Modeling long-range interactions without attention. *arXiv preprint arXiv:2102.08602*, 2021.
- [2] Luisa Bentivogli, Peter Clark, Ido Dagan, and Danilo Giampiccolo. The fifth pascal recognizing textual entailment challenge. In *TAC*, 2009.
- [3] Lucas Beyer, Olivier J Hénaff, Alexander Kolesnikov, Xiaohua Zhai, and Aäron van den Oord. Are we done with imagenet? *arXiv preprint arXiv:2006.07159*, 2020.
- [4] Andrew Brock, Soham De, Samuel L Smith, and Karen Simonyan. High-performance large-scale image recognition without normalization. *arXiv preprint arXiv:2102.06171*, 2021.
- [5] Tom B Brown, Benjamin Mann, Nick Ryder, Melanie Subbiah, Jared Kaplan, Prafulla Dhariwal, Arvind Neelakantan, Pranav Shyam, Girish Sastry, Amanda Askell, et al. Language models are few-shot learners. *arXiv preprint arXiv:2005.14165*, 2020.
- [6] Nicolas Carion, Francisco Massa, Gabriel Synnaeve, Nicolas Usunier, Alexander Kirillov, and Sergey Zagoruyko. End-to-end object detection with transformers. *arXiv preprint arXiv:2005.12872*, 2020.
- [7] Daniel Cer, Mona Diab, Eneko Agirre, Iñigo Lopez-Gazpio, and Lucia Specia. SemEval-2017 task 1: Semantic textual similarity multilingual and crosslingual focused evaluation. In *Proceedings of the 11th International Workshop on Semantic Evaluation (SemEval-2017)*, pages 1–14, Vancouver, Canada, August 2017. Association for Computational Linguistics.
- [8] Chun-Fu Chen, Quanfu Fan, and Rameswar Panda. Crossvit: Cross-attention multi-scale vision transformer for image classification. *arXiv preprint arXiv:2103.14899*, 2021.
- [9] Hanting Chen, Yunhe Wang, Tianyu Guo, Chang Xu, Yiping Deng, Zhenhua Liu, Siwei Ma, Chunjing Xu, Chao Xu, and Wen Gao. Pre-trained image processing transformer. *arXiv preprint arXiv:2012.00364*, 2020.
- [10] Zihan Chen, Hongbo Zhang, Xiaoji Zhang, and Leqi Zhao. Quora question pairs, 2018.
- [11] Kevin Clark, Minh-Thang Luong, Quoc V Le, and Christopher D Manning. Electra: Pre-training text encoders as discriminators rather than generators. *arXiv preprint arXiv:2003.10555*, 2020.
- [12] Ido Dagan, Oren Glickman, and Bernardo Magnini. The pascal recognising textual entailment challenge. In *Machine Learning Challenges Workshop*, pages 177–190. Springer, 2005.
- [13] Zhigang Dai, Bolun Cai, Yugeng Lin, and Junying Chen. Up-detr: Unsupervised pre-training for object detection with transformers. *arXiv preprint arXiv:2011.09094*, 2020.
- [14] Stéphane d’Ascoli, Hugo Touvron, Matthew Leavitt, Ari Morcos, Giulio Biroli, and Levent Sagun. Convit: Improving vision transformers with soft convolutional inductive biases. *arXiv preprint arXiv:2103.10697*, 2021.
- [15] Jia Deng, Wei Dong, Richard Socher, Li-Jia Li, Kai Li, and Li Fei-Fei. Imagenet: A large-scale hierarchical image database. In *2009 IEEE conference on computer vision and pattern recognition*, pages 248–255. Ieee, 2009.
- [16] Jacob Devlin, Ming-Wei Chang, Kenton Lee, and Kristina Toutanova. Bert: Pre-training of deep bidirectional transformers for language understanding. *arXiv preprint arXiv:1810.04805*, 2018.
- [17] William B. Dolan and Chris Brockett. Automatically constructing a corpus of sentential paraphrases. In *Proceedings of the Third International Workshop on Paraphrasing (IWP2005)*, 2005.
- [18] Yihe Dong, Jean-Baptiste Cordonnier, and Andreas Loukas. Attention is not all you need: Pure attention loses rank doubly exponentially with depth. *arXiv preprint arXiv:2103.03404*, 2021.
- [19] Alexey Dosovitskiy, Lucas Beyer, Alexander Kolesnikov, Dirk Weissenborn, Xiaohua Zhai, Thomas Unterthiner, Mostafa Dehghani, Matthias Minderer, Georg Heigold, Sylvain Gelly, et al. An image is worth 16x16 words: Transformers for image recognition at scale. *arXiv preprint arXiv:2010.11929*, 2020.
- [20] Danilo Giampiccolo, Bernardo Magnini, Ido Dagan, and Bill Dolan. The third pascal recognizing textual entailment challenge. In *Proceedings of the ACL-PASCAL workshop on textual entailment and paraphrasing*, pages 1–9. Association for Computational Linguistics, 2007.

- [21] Chengyue Gong, Dilin Wang, Meng Li, Vikas Chandra, and Qiang Liu. Improve vision transformers training by suppressing over-smoothing. *arXiv preprint arXiv:2104.12753*, 2021.
- [22] Meng-Hao Guo, Jun-Xiong Cai, Zheng-Ning Liu, Tai-Jiang Mu, Ralph R Martin, and Shi-Min Hu. Pct: Point cloud transformer. *arXiv preprint arXiv:2012.09688*, 2020.
- [23] R Bar Haim, Ido Dagan, Bill Dolan, Lisa Ferro, Danilo Giampiccolo, Bernardo Magnini, and Idan Szpektor. The second pascal recognising textual entailment challenge. In *Proceedings of the Second PASCAL Challenges Workshop on Recognising Textual Entailment*, 2006.
- [24] Kai Han, An Xiao, Enhua Wu, Jianyuan Guo, Chunjing Xu, and Yunhe Wang. Transformer in transformer. *arXiv preprint arXiv:2103.00112*, 2021.
- [25] Kaiming He, Xiangyu Zhang, Shaoqing Ren, and Jian Sun. Deep residual learning for image recognition. In *Proceedings of the IEEE conference on computer vision and pattern recognition*, pages 770–778, 2016.
- [26] Andrew G Howard, Menglong Zhu, Bo Chen, Dmitry Kalenichenko, Weijun Wang, Tobias Weyand, Marco Andreetto, and Hartwig Adam. Mobilenets: Efficient convolutional neural networks for mobile vision applications. *arXiv preprint arXiv:1704.04861*, 2017.
- [27] Zihang Jiang, Qibin Hou, Li Yuan, Daquan Zhou, Xiaojie Jin, Anran Wang, and Jiashi Feng. Token labeling: Training a 85.4% top-1 accuracy vision transformer with 56m parameters on imagenet. *arXiv preprint arXiv:2104.10858*, 2021.
- [28] Simon Kornblith, Mohammad Norouzi, Honglak Lee, and Geoffrey Hinton. Similarity of neural network representations revisited. In *International Conference on Machine Learning*, pages 3519–3529. PMLR, 2019.
- [29] Zhenzhong Lan, Mingda Chen, Sebastian Goodman, Kevin Gimpel, Piyush Sharma, and Radu Soricut. ALBERT: A lite bert for self-supervised learning of language representations. *arXiv preprint arXiv:1909.11942*, 2019.
- [30] Hector Levesque, Ernest Davis, and Leora Morgenstern. The winograd schema challenge. In *Thirteenth International Conference on the Principles of Knowledge Representation and Reasoning*, 2012.
- [31] Jianan Li, Xiaodan Liang, ShengMei Shen, Tingfa Xu, Jiashi Feng, and Shuicheng Yan. Scale-aware fast r-cnn for pedestrian detection. *IEEE transactions on Multimedia*, 20(4):985–996, 2017.
- [32] Yawei Li, Kai Zhang, Jiezhong Cao, Radu Timofte, and Luc Van Gool. Localvit: Bringing locality to vision transformers. *arXiv preprint arXiv:2104.05707*, 2021.
- [33] Pengfei Liu, Xipeng Qiu, and Xuanjing Huang. Recurrent neural network for text classification with multi-task learning. *arXiv preprint arXiv:1605.05101*, 2016.
- [34] Ze Liu, Yutong Lin, Yue Cao, Han Hu, Yixuan Wei, Zheng Zhang, Stephen Lin, and Baining Guo. Swin transformer: Hierarchical vision transformer using shifted windows. *arXiv preprint arXiv:2103.14030*, 2021.
- [35] Wenjie Luo, Yujia Li, Raquel Urtasun, and Richard Zemel. Understanding the effective receptive field in deep convolutional neural networks. *arXiv preprint arXiv:1701.04128*, 2017.
- [36] Adam Paszke, Sam Gross, Francisco Massa, Adam Lerer, James Bradbury, Gregory Chanan, Trevor Killeen, Zeming Lin, Natalia Gimelshein, Luca Antiga, et al. Pytorch: An imperative style, high-performance deep learning library. In *Advances in neural information processing systems*, pages 8026–8037, 2019.
- [37] Zhiliang Peng, Wei Huang, Shanzhi Gu, Lingxi Xie, Yaowei Wang, Jianbin Jiao, and Qixiang Ye. Conformer: Local features coupling global representations for visual recognition. *arXiv preprint arXiv:2105.03889*, 2021.
- [38] Alec Radford, Karthik Narasimhan, Tim Salimans, and Ilya Sutskever. Improving language understanding by generative pre-training, 2018.
- [39] Pranav Rajpurkar, Jian Zhang, Konstantin Lopyrev, and Percy Liang. SQuAD: 100,000+ questions for machine comprehension of text. In *Proceedings of the 2016 Conference on Empirical Methods in Natural Language Processing*, pages 2383–2392, Austin, Texas, November 2016. Association for Computational Linguistics.
- [40] Hasim Sak, Andrew W Senior, and Françoise Beaufays. Long short-term memory recurrent neural network architectures for large scale acoustic modeling. 2014.

- [41] Mark Sandler, Andrew Howard, Menglong Zhu, Andrey Zhmoginov, and Liang-Chieh Chen. Mobilenetv2: Inverted residuals and linear bottlenecks. In *Proceedings of the IEEE conference on computer vision and pattern recognition*, pages 4510–4520, 2018.
- [42] Noam Shazeer, Zhenzhong Lan, Youlong Cheng, Nan Ding, and Le Hou. Talking-heads attention. *arXiv preprint arXiv:2003.02436*, 2020.
- [43] Richard Socher, Alex Perelygin, Jean Wu, Jason Chuang, Christopher D Manning, Andrew Y Ng, and Christopher Potts. Recursive deep models for semantic compositionality over a sentiment treebank. In *Proceedings of the 2013 conference on empirical methods in natural language processing*, pages 1631–1642, 2013.
- [44] Kihyuk Sohn and Honglak Lee. Learning invariant representations with local transformations. *arXiv preprint arXiv:1206.6418*, 2012.
- [45] Aravind Srinivas, Tsung-Yi Lin, Niki Parmar, Jonathon Shlens, Pieter Abbeel, and Ashish Vaswani. Bottleneck transformers for visual recognition. *arXiv preprint arXiv:2101.11605*, 2021.
- [46] Mingxing Tan and Quoc V Le. Efficientnet: Rethinking model scaling for convolutional neural networks. *arXiv preprint arXiv:1905.11946*, 2019.
- [47] Yi Tay, Dara Bahri, Donald Metzler, Da-Cheng Juan, Zhe Zhao, and Che Zheng. Synthesizer: Rethinking self-attention in transformer models. *arXiv preprint arXiv:2005.00743*, 2020.
- [48] Hugo Touvron, Matthieu Cord, Matthijs Douze, Francisco Massa, Alexandre Sablayrolles, and Hervé Jégou. Training data-efficient image transformers & distillation through attention. *arXiv preprint arXiv:2012.12877*, 2020.
- [49] Hugo Touvron, Matthieu Cord, Alexandre Sablayrolles, Gabriel Synnaeve, and Hervé Jégou. Going deeper with image transformers. *arXiv preprint arXiv:2103.17239*, 2021.
- [50] Hugo Touvron, Andrea Vedaldi, Matthijs Douze, and Hervé Jégou. Fixing the train-test resolution discrepancy. *arXiv preprint arXiv:1906.06423*, 2019.
- [51] Ashish Vaswani, Noam Shazeer, Niki Parmar, Jakob Uszkoreit, Llion Jones, Aidan N Gomez, Łukasz Kaiser, and Illia Polosukhin. Attention is all you need. *Advances in neural information processing systems*, 30:5998–6008, 2017.
- [52] Alex Wang, Amanpreet Singh, Julian Michael, Felix Hill, Omer Levy, and Samuel R Bowman. Glue: A multi-task benchmark and analysis platform for natural language understanding. *arXiv preprint arXiv:1804.07461*, 2018.
- [53] Fei Wang, Mengqing Jiang, Chen Qian, Shuo Yang, Cheng Li, Honggang Zhang, Xiaogang Wang, and Xiaoou Tang. Residual attention network for image classification. In *Proceedings of the IEEE conference on computer vision and pattern recognition*, pages 3156–3164, 2017.
- [54] Yuqing Wang, Zhaoliang Xu, Xinlong Wang, Chunhua Shen, Baoshan Cheng, Hao Shen, and Huaxia Xia. End-to-end video instance segmentation with transformers. *arXiv preprint arXiv:2011.14503*, 2020.
- [55] Alex Warstadt, Amanpreet Singh, and Samuel R Bowman. Neural network acceptability judgments. *Transactions of the Association for Computational Linguistics*, 7:625–641, 2019.
- [56] Ross Wightman. Pytorch image models. <https://github.com/rwightman/pytorch-image-models>, 2019.
- [57] Adina Williams, Nikita Nangia, and Samuel Bowman. A broad-coverage challenge corpus for sentence understanding through inference. In *Proceedings of the 2018 Conference of the North American Chapter of the Association for Computational Linguistics: Human Language Technologies, Volume 1 (Long Papers)*, pages 1112–1122, New Orleans, Louisiana, June 2018. Association for Computational Linguistics.
- [58] Saining Xie, Ross Girshick, Piotr Dollár, Zhuowen Tu, and Kaiming He. Aggregated residual transformations for deep neural networks. In *Proceedings of the IEEE conference on computer vision and pattern recognition*, pages 1492–1500, 2017.
- [59] Fuzhi Yang, Huan Yang, Jianlong Fu, Hongtao Lu, and Baining Guo. Learning texture transformer network for image super-resolution. In *Proceedings of the IEEE/CVF Conference on Computer Vision and Pattern Recognition*, pages 5791–5800, 2020.

- [60] Li Yuan, Yunpeng Chen, Tao Wang, Weihao Yu, Yujun Shi, Francis EH Tay, Jiashi Feng, and Shuicheng Yan. Tokens-to-token vit: Training vision transformers from scratch on imagenet. *arXiv preprint arXiv:2101.11986*, 2021.
- [61] Li Yuan, Francis EH Tay, Guilin Li, Tao Wang, and Jiashi Feng. Revisiting knowledge distillation via label smoothing regularization. In *Proceedings of the IEEE/CVF Conference on Computer Vision and Pattern Recognition*, pages 3903–3911, 2020.
- [62] Yanhong Zeng, Jianlong Fu, and Hongyang Chao. Learning joint spatial-temporal transformations for video inpainting. In *European Conference on Computer Vision*, pages 528–543. Springer, 2020.
- [63] Hengshuang Zhao, Li Jiang, Jiaya Jia, Philip Torr, and Vladlen Koltun. Point transformer. *arXiv preprint arXiv:2012.09164*, 2020.
- [64] Minghang Zheng, Peng Gao, Xiaogang Wang, Hongsheng Li, and Hao Dong. End-to-end object detection with adaptive clustering transformer. *arXiv preprint arXiv:2011.09315*, 2020.
- [65] Daquan Zhou, Xiaojie Jin, Qibin Hou, Kaixin Wang, Jianchao Yang, and Jiashi Feng. Neural epitome search for architecture-agnostic network compression. In *International Conference on Learning Representations*, 2019.
- [66] Daquan Zhou, Bingyi Kang, Xiaojie Jin, Linjie Yang, Xiaochen Lian, Qibin Hou, and Jiashi Feng. Deepvit: Towards deeper vision transformer. *arXiv preprint arXiv:2103.11886*, 2021.
- [67] Luwei Zhou, Yingbo Zhou, Jason J Corso, Richard Socher, and Caiming Xiong. End-to-end dense video captioning with masked transformer. In *Proceedings of the IEEE Conference on Computer Vision and Pattern Recognition*, pages 8739–8748, 2018.
- [68] Xizhou Zhu, Weijie Su, Lewei Lu, Bin Li, Xiaogang Wang, and Jifeng Dai. Deformable detr: Deformable transformers for end-to-end object detection. *arXiv preprint arXiv:2010.04159*, 2020.

A More implementation details

A.1 Training hyper-parameters

For all the ablation experiments, we use the standard training recipe [56] that is used for reproducing the ViT baselines. When comparing with other state-of-the-art (SOTA) methods, we adopt the advanced training recipe as proposed in [27]. Their detailed configurations are shown in Tab. 8. We train all models with 8 NVIDIA Telsa-V100 GPUs.

Table 8: Default training hyper-parameters for our experiments.

H-param.	Standard	Advanced
Epoch	300	300
Batch size	256	512
LR	$5e-3 \cdot \frac{\text{batch_size}}{256}$	$5e-3 \cdot \frac{\text{batch_size}}{512}$
LR decay	cosine	cosine
Weight decay	0.05	0.05
Warmup epochs	5	5
Dropout	0	0
Stoch. Depth	0.1	$0.1 \cdot \frac{\#\text{Blocks}}{12}$
MixUp	0.2	0.8
CutMix	0	1.0
Erasing prob.	0.25	0.25
RandAug	9/0.5	9/0.5

A.2 Fine-tuning with larger image resolutions

On ImageNet, all models are trained from scratch with image resolution of 224×224 . When compare with other SOTA models, we fine-tune the models with larger image resolutions using the same fine-tuning procedures as adopted in [48]. As larger image resolutions have more positional embeddings, we interpolate the positional encodings in the same manner as the one proposed in [19].

A.3 Model configurations of Refiner-ViT

As discussed in [60], a deep and narrow neural network typically is more efficient than a wide and shallow one. To verify this, we conduct a pair of experiments using these two architecture configurations respectively and the results are shown in Tab. 9. It is clearly observed that with comparable classification accuracy, a deep and narrow network takes 71% less number of parameters.

Table 9: Comparison of the deep-narrow and shallow-wide architecture configurations.

Model	#Blocks	Hidden dim	#Heads	Params	Top-1 (%)
Refined-ViT	12	768	12	86M	83.1
Refined-ViT	16	384	12	25M	83.0

Thus, we design the architecture of Refiner-ViT based on the same deep and narrow network architecture. The detailed configurations and the comparison with the ViT-base architecture are shown in Tab. 10.

A.4 Feature evolving speed and feature similarity with CKA

As shown in Fig. 2 and Fig. 4 in the main paper, we compare the similarity between the intermediate token features at the output of each block and the final layer, normalized by the similarity between the first layer’s output features and the final output features as shown in Eqn. (2):

$$F_k = \frac{CKA(f_k, f_{out})}{CKA(f_{in}, f_{out})}, \quad (2)$$

Table 10: Model architecture configurations.

Model	#Blocks	Hidden dim	#Head	#Params	Training Resolution
Refined-ViT-Base	12	768	12	86M	224
Refined-ViT-S	16	384	12	25M	224
Refined-ViT-M	32	420	12	55M	224
Refined-ViT-L	32	512	16	81M	224

where f_k denotes the token features at layer k , f_{in} denotes the token features at the first transformer block and f_{out} denotes the features at the final output of the model. The metric CKA is calculated with linear kernel function as proposed in [28]. The batch size is set to be 32. The similarity score at the output of each block is an average of ten runs with randomly sampled image batches.

B More experiments

B.1 Performance improvements of refiner under different training techniques

As shown in DeiT [48], more complex augmentations and fine-tuned training recipe could improve the performance of ViTs significantly without architecture changes. We run a set of experiments to show that the improvements brought by refiner is orthogonal to the training recipes to some extent. We select two training recipes for comparison. The first one uses the searched learning rate schedule and data augmentation policy as proposed in [48]. The second one uses the more complicated patch processing as proposed in [60]. As shown in Tab. 11, under different training settings, the improvements from the refiner are all significant on ImageNet.

Table 11: Performance gain from refiner under different training recipes.

Training techniques	#Param.	Original Top-1 (%)	+ Refined-ViT
Baseline (ViT-Base)	86M	79.3	81.2 (+1.9)
+ DeiT-Base ([48])	86M	81.5	82.3 (+0.8)
+ More convs for patch embedding	86M	82.2	83.1 (+0.9)

B.2 Impacts of the attention heads

As discussed in [49], increasing the number of attention heads will reduce the embedding dimension per head and thus degrade the network performance. Differently, refiner expands the number of heads with a linear projection function. With the implementation of the linear projection, refiner will keep each head’s embedding dimension unchanged. As shown in Tab. 12, the performance keeps increasing with Refined-ViT.

Table 12: Ablation on the impact of the number of the heads for ViT-Small with 16 blocks and 384 embedding dimension. We report top-1 accuracy on ImageNet. The accuracy for ViT-Small with different head numbers are adopted from [49].

# Heads	ViT-Small	Refined-ViT
8	79.9	82.5
12	80.0	82.6
16	80.0	82.8

B.3 Impacts of the kernel size

For all the experiments in the main paper, the convolution kernel is set to be 3×3 by default. In Fig. 6, we show the classification results on ImageNet with different kernel size. It is observed that all

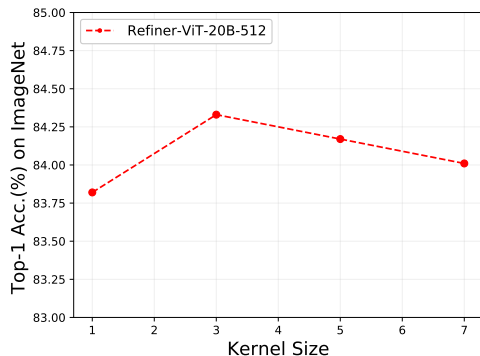


Figure 6: Top-1 classification accuracy of Refined-ViT with different local kernel sizes.

kernels achieve much better accuracy than the baseline method (kernel size of 1) and the refiner with kernel size 3 achieves that highest accuracy. This further verify that attention reinforcement within the local area could improve the performance of ViTs.

B.4 Refiner makes the attention maps shareable

Table 13: Ablation on the number of shared attention maps on ViT-16B with 384 embedding dimension.

#Shared Blocks	SA	Refiner
0	82	83.0
1	77	83.0
2	70	82.8
3	NAN	82.6

Refiner enables the attention maps to capture some critical spatial relation among the tokens. To see this, we compute the attention maps with Refiner and let the following a number of blocks to reuse such pre-computed attention maps. The results are given in Tab. 13. Interestingly we find that the attention maps after Refiner can be shared (reused) by several following SA blocks. Let the directly adjacent SA block reuse the refined attention map from the previous block will maintain the model overall performance. Sharing the attention maps with the following two SA blocks only drop the accuracy by 0.2%. In stark contrast, the attention maps from the vanilla SA are completely not shareable, leading the model performance to drop severely. This demonstrates Refiner is effective at extracting useful patterns and this finding is also in accordance with the one from a recent NLP study [47]. Therefore, across the experiments with Refiner, we shared the attention maps for 1 adjacent transformer block.

C Dataset description for NLP experiments

GLUE benchmark [52] is a collection of nine natural language understanding tasks where the labels of the testing set is hidden and the researchers need to submit their predictions to the evaluation server³ to obtain results on testing sets. In this work, we only present results of single-task setting for fair comparison. The nine tasks included in GLUE benchmark are described in details as below.

MNLI The Multi-Genre Natural Language Inference Corpus [57] is a dataset of sentence pairs with textual entailment annotations. Given a premise sentence and a hypothesis sentence, the task is to predict their relationships including ENTENTAILMENT, CONTRADICTION and NEUTRAL. The data is collected from ten distinct genres including both written and spoken English.

³<https://gluebenchmark.com>

QNLI Question Natural Language Inference is a binary sentence pair classification task, converted from The Stanford Question Answering Dataset [39] (a question-answering dataset). Each sample of QNLI contains a context sentence and a question. The task is to determine whether the context sentence contains the answer to the question.

QQP The Quora Question Pairs dataset [10] is a collection of question pairs from Quora (a community question-answering website). The task is to determine whether the two questions in a pair are semantically equivalent.

RTE Similar to MNLI, the Recognizing Textual Entailment (RTE) dataset is also a binary classification task, i.e., *entailment* and *not entailment*. It is from a series of annual textual entailment challenges including RTE1 [12], RTE2 [23], RTE3 [20], and RTE5 [2].

SST-2 The Stanford Sentiment Treebank [43] consists of sentences from movie reviews and human annotations of their sentiment. GLUE uses the two-way (POSITIVE/NEGATIVE) class split.

MRPC The Microsoft Research Paraphrase Corpus [17] contains data from online news that consists of sentence pairs with human annotations regarding whether the sentences in the pair are semantically equivalent.

CoLA The Corpus of Linguistic Acceptability [55] is a binary single-sentence classification dataset containing the examples annotated with whether it is a grammatical English sentence.

SST-B The Semantic Textual Similarity Benchmark [7] is a collection of human-annotated sentence pairs with a similarity score ranging from 1 to 5. The target is to predict the scores with a given sentence.

WNLI Winograd NLI [30] is a small natural language inference dataset. However, as highlighted on the GLUE web page⁴, there are issues with the construction of it. Thus following the practice of previous works (GPT [38] and BERT [29] etc.), we exclude this dataset for a fair comparison.

⁴<https://gluebenchmark.com/faq>